Interactive Real-Time Simulation of Robotic Snap Connection Process

Minji Lee, Jeongmin Lee, Jaemin Yoon and Dongjun Lee[†]

Abstract— We propose a novel real-time physically-accurate simulation framework for the snap connection process. For this, we first notice the peculiarities of the process, namely, small/smooth deformation, stiff connector, and segmented contact. We then design our simulation to fully exploit these peculiarities by adopting the following strategies: 1) linear finite element method (FEM [1]) modeling, which is adequate to deal with the small snap connector deformation while providing much faster speed as compared to nonlinear FEM; 2) reducing the dimension by balanced model reduction (BMR [2]) and geometrical segmentation of the snap connector FEM model; 3) parallelized data-driven collision detection, which turns out to further significantly speed up our simulation. Experimentally verified simulations are also performed to show the efficacy of our proposed simulation framework.

Video: https://youtu.be/s3sfPFIPS2c

I. INTRODUCTION

With the recent advancements of robotics technologies, many attempts have been made to bring the robots into real-world applications including the snap connection process. This process is not only important for robotic manufacturing/assembly (e.g., plastic switch box assembly, inserting LAN cable, etc.), but also for household robotics (e.g., tidying objects with snap-belts, placing dishwasher stopper, etc.) - see Fig. 1. Fast and physically accurate simulation of the snap connectors would then be useful for the development of its control strategies. Since model-based control of robots interacting with soft object or soft robot is complicated due to its high degree of freedom ([3], [4]), data-driven reinforcement learning(RL) receives lots of attention, which typically requires a vast number of simulation data. Its real-time simulation would even allow for the haptic rendering of the snap connection in virtual reality (VR [5]) or the development of shared-autonomy RL strategy for the snap connection.

In this paper, we develop a novel *real-time physically-accurate* simulation framework for this snap connection process. We then render our simulation framework to exploit the peculiarities of the snap connection processes s.t.,: 1) we choose linear finite element method (FEM [1]) instead of nonlinear FEM [6], as it is enough to deal with the small deformation of snap connection while providing much faster speed; 2) we reduce the dimension of dynamics by
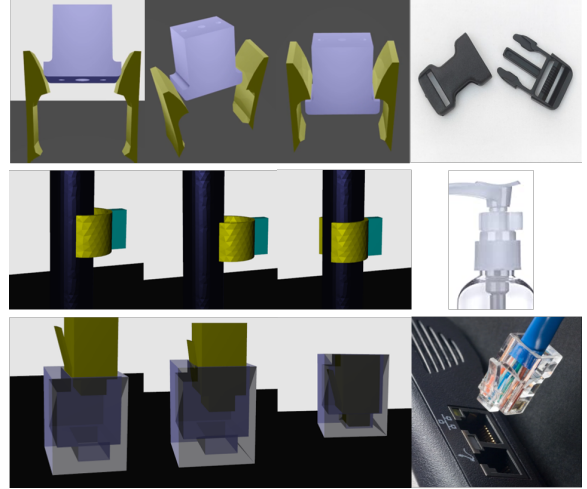
Fig. 1: Simulation snapshots of various real-world snap connection processes

geometrically segmenting the snap connector FEM model into few segments and adopting the balanced model reduction (BMR [2]) to further reduce the dimension of each segmented model; and 3) we devise a parallelized data-driven collision detection module between the connector surfaces in the form of multi layer perceptron (MLP [7]) and with the help of graphics processing unit (GPU), which turns out to further significantly speed up the simulation.

Our proposed framework can real-time simulate the fast snap closing motion while not requiring any *prior* experiments/simulations for the model reduction (thanks to the adoption of BMR). Unlike other sate-of-the-art results (e.g., [6], [8], [9]), it does not rely on implicit euler integration, which is well-known to increase the damping effect in the simulation [10], it can simulate the fast snap closing motion.

II. SEGMENTATION WITH MODEL REDUCTION

A. Segmentation of Socket Connector

The socket connector FEM model is segmented into the nodes with possible contact and the nodes with no contact (e.g., internal nodes). Define $x_1 := [x_{11}; x_{12}; \cdots; x_{1n_1}]^T \in \mathbb{R}^{3n_1}, x_2 := [x_{21}; x_{22}; \cdots; x_{2n_2}]^T \in \mathbb{R}^{3n_2}$, where x_1, x_2 denote the nodes of the two segments with x_1 being the nodes with possible contacts, while x_2 not. Then, when discretizing via passive midpoint method (PMI [10]), the representative velocity of i-th segment $\hat{v}_{i,k}$ for the time duration $t \in [T_k, T_{k+1}]$, can be written as:

$$\hat{v}_{i,k} = \hat{M}_i^{-1} \left(\lambda_{i,k} + f_{i,c,k} \right) + v_{i,f,k} \qquad (1)$$

(a) Plastic buckle-like geometry

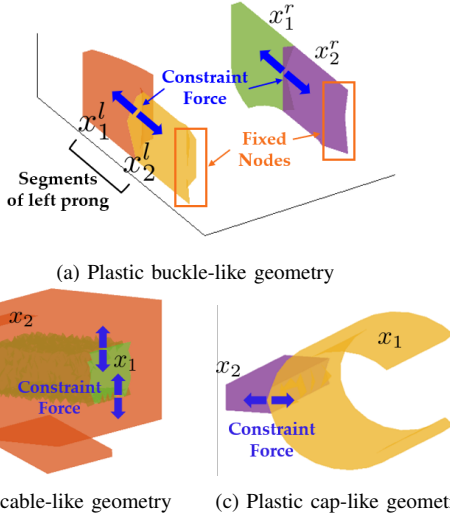(b) Lan cable-like geometry   (c) Plastic cap-like geometry

Fig. 2: Segmentation structure of the socket connectors for various geometry

where $v_{i,f,k} := \hat{M}_i^{-1}\left(\frac{2M_i}{T}v_{i,k} - K_i x_{i,k}\right)$ and $\hat{M}_i := \frac{2M_i}{T} + D_i + K_i\frac{T}{2}$, T is the time step, $\lambda_i \in \mathbb{R}^{n_i}$ is the constraint force of the i-th segment to ensure the joining between the two segments, $f_{i,c}$ is the contact force and $M_i, D_i, K_i \in \mathbb{R}^{3n_i \times 3n_i}$ are mass, damping, stiffness matrix of each FEM segments. Since there is no contact on second segment, the contact force of the second segment is zero: $f_{2,c,k} = 0$.

We also design the constraint force λ_i as a strong PMI-based spring-damper connection between coupling nodes. Thanks to our adoption of PMI for the simulation, we can choose arbitrarily large spring, damping coefficient for the (virtually-rigid) segmental coupling without losing stability nor real-timeness, even with zero damping(D_i) or BMR. This spring-based segmentation is equivalent to the original FEM model if the constraints are strictly satisfied. Since our system is passive even when the spring coefficient between coupling nodes k_c are large, we can effectively ensure the tight connectivity by increasing k_c, which makes the solution close to the original problem.

We analytically eliminate the coupling $\lambda_{i,k}$, thereby, speeding up the simulation. By substituting and simplifying the equations, the dynamics of the socket connector can be written as follow:

$$\hat{v}_{1,k} = A f_{1,c,k} + v_{1,f,k}, \quad \hat{v}_{2,k} = A_2 \hat{v}_{1,k} + v_{2,f,k} \quad (2)$$

where $A \in \mathbb{R}^{3n_1 \times 3n_1}, A_2 \in \mathbb{R}^{3n_2 \times 3n_1}$ denotes the mapping matrix and $v_{1,f,k}, v_{2,f,k}$ are the remaining term, which physical meaning is the velocity when $f_{1,c,k} = 0$ and $\hat{v}_{1,k} = 0$ respectively. Here, since the mapping matrix A, A_2 is a time-invariant constant matrix, it can be pre-computed. As the large-dimensional state update equation is split into two equations with smaller dimension via segmentation, parallelization is made possible and the computation time is reduced. Recall that the segment without contact can be segmented even further so that the effectiveness can be increased.

B. Segmentation with Balanced Model Reduction

By conducting BMR ([2]) for each segment, the dimension of the states can be further reduced and thus speeding up the computation. As a result of BMR on each segement, the reduced state $z_i \in \mathbb{R}^{n_i^r}$ can be described as linear mapping of the full order state x_i. Then the state update equation (1) and constraint force can be rewritten for the reduced state z_i. By following the same steps outlined above, $\dot{\hat{z}}_{1,k}$ and $\dot{\hat{z}}_{2,k}$ can be written likewise as:

$$\dot{\hat{z}}_{2,k} = B_1 \dot{\hat{z}}_{1,k} + \dot{z}_{2,f,k} \quad (3)$$

$$\dot{\hat{z}}_{1,k} = B_2 f_{1,c,k} + \dot{z}_{1,f,k} \quad (4)$$

where $B_1 \in \mathbb{R}^{n_2^r \times n_1^r}$ and $B_2 \in \mathbb{R}^{n_2^r \times 3n_1}$ are constant matrices, which can be precalculated. In addition to the advantage of being split into dynamics equations of small dimensions that can be parallelized, the dimensions of the state variables have further decreased from $3n_i$ to n_i^r, which improves the computational speed. It can be analytically proved that our segmentation with BMR method strictly satisfies discrete time passivity without any artificial damping.

III. CONTACT HANDLING

A. MLP-based Collision Detection

To reduce the computation time at collision detection stage, we develop a multi layer perceptron (MLP) based collision detection technique. We approximate the distance function from an arbitrary point to the given mesh into MLP so that the complex collision detection algorithm can be simplified into a neural network traversal process consisting of simple calculations.

The MLP is trained with numerous randomly generated points and their distance function values, which can be computed as the minimum signed distance value from the triangle on the surface of the plug connector to the point.

At every time step, a number of points $\bar{p} = [p_1; \cdots; p_N]$ are obtained by interpolating FEM nodes of the socket connector (i.e., $x_{1,k} \in \mathbb{R}^{3n_1}$) and these points pass through MLP, and the distance function value of each point $d = [d_1, \cdots, d_N]$ can be achieved. With the sign of the values, the contact points can be chosen. Moreover, since the normal vectors can be obtained by the gradients of the signed distance functions, the normal vectors of the contact points can be achieved by passing through the differentiated MLP.

B. Contact Solver

The next step is to calculate the contact force on the obtained contact points. We compute the contact force that satisfies Coulomb's friction and velocity-level Signorini condition based on the maximal dissipation principle [11]. In the case of the snap connection process, since the contact force is applied from two symmetrical directions, the condition of the Delassus operator is bad and PGS method does not converge well. As an alternative, we use maximal dissipation algorithm which finds the contact force that maximizes the dissipation. The contact problem can then be written as optimization that maximizes energy dissipation, which formulation is concurrent with PMI.
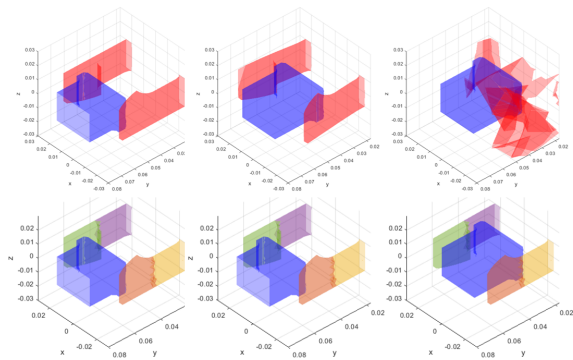
Fig. 3: Snapshots of the simulation results: nonlinear FEM (with geometric nonlinearity and linear material) (top) and proposed framework (bottom).
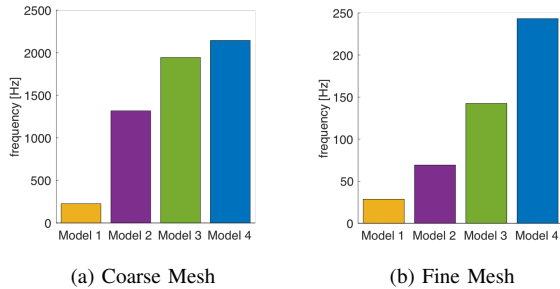

(a) Coarse Mesh   (b) Fine Mesh

Fig. 4: Frequency comparison between 4 models - Model 1: original FEM model; Model 2: original FEM model with GPU collision detection; Model 3: Model 2 with segmentation; and Model 4: Model 3 with BMR.

IV. SIMULATION ANALYSIS

A. Stability Under High Stiffness

To show the better stability property of our linear FEM based simulator, we compare the simulation with that of the nonlinear geometry FEM, both with high Young's modulus. Our framework can stably simulate the snap connection behavior even when the damping term is removed. Unlike our framework, if the material is very stiff (i.e., high Young's modulus), typically linearized dynamics of the nonlinear FEM diverges even with small artificial damping, due to the dynamics linearization error regardless of the integration method as shown in Fig. 3.

B. Computation Time Analysis

We analyze the computation time of our proposed simulator and how effective each of the adopted ideas speed up the simulation. As the result of segmentation and BMR, the dimension of the original FEM model is reduced from 663 to 6 and 25 (for each segment) when discretized coarsely and from 1266 to 6 and 96 when discretized finely.

With the reduction of the dimension and the accelerated collision detection, the simulation frequency (i.e. number of time steps calculated in 1 second) was increased by 8.5-9.5 times faster for different size of meshes. Fig. 4 shows the frequency of the simulation of each model. Exploiting data-driven collision detection, segmentation and BMR has enhanced the simulation frequency. In the case of the coarse mesh, data-driven collision detection affected the simulation time remarkably, whereas in the case of the fine mesh, the effect of segmentation and reduction was huge.
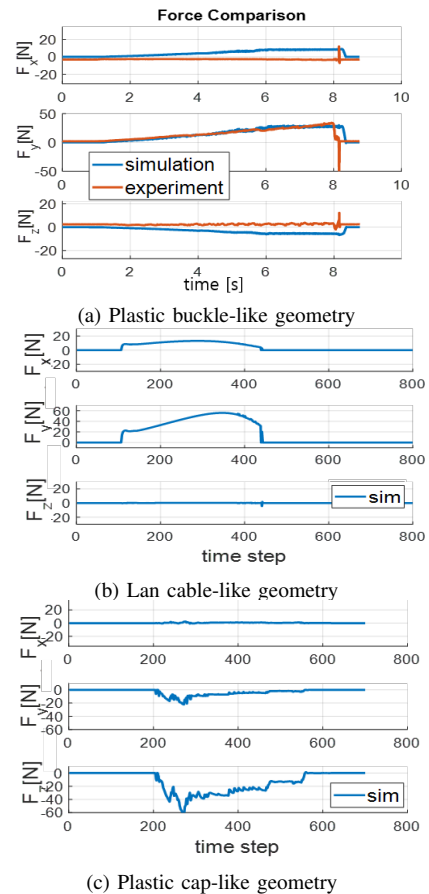

(a) Plastic buckle-like geometry

(b) Lan cable-like geometry

(c) Plastic cap-like geometry

Fig. 5: Force result for various materials and geometries

C. Simulation Result with Experimental Data

To verify the framework, we compare the experiment results with the simulations. The simulation is performed using the same control input (i.e. desired position of the plug connector) and material parameters (i.e. Poisson's ratio and Young's modulus) with the experiment. Here, time step is used as $1[ms]$. With the force/torque sensor attached below the socket connector, we measure the force exerted to the floor and compare it with the calculated force in simulation.

Fig. 5 illustrates the comparison of the measured force from the experiment and that calculated from proposed simulation. The root mean square error of the norm of the force was $4.9355[N]$, where the maximum force was $48.1588[N]$. Also for different geometries and material properties, reasonable contact force was deduced as shown in Fig.5.

V. CONCLUSION

We present a real-time snap connection framework that matches with real-world physics. For this, segmentation and BMR are conducted to reduce the dimension of the states. Moreover, data-driven collision detection using GPU parallelization is proposed to speed up the detection. As a result, we achieve the frequency of the simulation up to $2.2kHz$. The devised framework is then verified through comparison with the experiment and it is confirmed that the accuracy was not lost in the process of reduction.

REFERENCES

[1] T. JR Hughes. *The finite element method: linear static and dynamic finite element analysis*. Courier Corporation, 2012.

[2] J. Yoon, I. Hong, and D. Lee. Passive model reduction and switching for fast soft object simulation with intermittent contacts. In *IEEE/RSJ International Conference on Intelligent Robots and Systems*, pages 6963–6970, 2019.

[3] Z. Simon, P. Roi, and C. Stelian. Dynamic manipulation of deformable objects with implicit integration. *IEEE Robotics and Automation Letters*, 2021.

[4] B. James M, B. Pol, P. Roi, and C. Stelian. Trajectory optimization for cable-driven soft robot locomotion. In *Robotics: Science and Systems*, 2019.

[5] Y. Lee, M. Kim, Y. Lee, J. Kwon, Y. Park, and D. Lee. Wearable finger tracking and cutaneous haptic interface with soft sensors for multi-fingered virtual manipulation. *IEEE/ASME Transactions on Mechatronics*, 24(1):67–77, 2018.

[6] T. Belytschko, W. Liu, B. Moran, and K. Elkhodary. *Nonlinear finite elements for continua and structures*. John wiley & sons, 2013.

[7] S. Haykin. *Neural Networks and Learning Machines*. Pearson Education India, 2010.

[8] M. Ly, J. Jouve, L. Boissieux, and F. Bertails-Descoubes. Projective dynamics with dry frictional contact. *ACM Transactions on Graphics*, 39(4):57–1, 2020.

[9] M. Macklin, K. Erleben, M. Müller, N. Chentanez, S. Jeschke, and V. Makoviychuk. Non-smooth newton methods for deformable multi-body dynamics. *ACM Transactions on Graphics*, 38(5):1–20, 2019.

[10] M. Kim, Y. Lee, Y. Lee, and D. Lee. Haptic rendering and interactive simulation using passive midpoint integration. *International Journal of Robotics Research*, 36(12):1341–1362, 2017.

[11] T. Preclik, S. Eibl, and U. Rüde. The maximum dissipation principle in rigid-body dynamics with inelastic impacts. *Computational Mechanics*, 62(1):81–96, 2018.